Received: 11 May 2020 | Revised: 8 October 2020 | Accepted: 16 October 2020

DOI: 10.1002/jbm.a.37122

ORIGINAL ARTICLE

Society For Biomaterials | WILEY

# Effect of bioactive Biosilicate®/F18 glass scaffolds on osteogenic differentiation of human adipose stem cells

Claudia P. Marin[1] | Geovana L. Santana[1] | Meghan Robinson[2] | Stephanie M. Willerth[2] | Murilo C. Crovace[1] | Edgar D. Zanotto[1]

[1]CeRTEV–Center for Research, Technology, and Education in Vitreous Materials, Vitreous Materials Laboratory (LaMaV), Department of Materials Engineering (DEMA), Graduate Program in Materials Science and Engineering, Federal University of São Carlos (UFSCar), São Carlos, Brazil

[2]Department of Mechanical Engineering and Division of Medical Sciences, University of Victoria, Victoria, British Columbia, Canada

**Correspondence**
Claudia P. Marin, CeRTEV–Center for Research, Technology, and Education in Vitreous Materials, Vitreous Materials Laboratory (LaMaV), Department of Materials Engineering (DEMA), Graduate Program in Materials Science and Engineering, Federal University of São Carlos (UFSCar), São Carlos, Brazil.
Email: clapa.mar2012@gmail.com

**Funding information**
Coordination for the Improvement of Higher Education Personnel (CAPES); Emerging Leaders in the Americas Program (ELAP); São Paulo Research Foundation (FAPESP)

## Abstract

This study evaluated the gene expression profile of the human adipose-derived stem cells (hASCs) grown on the Biosilicate®/F18 glass (BioS-2P/F18) scaffolds. hASCs were cultured using the osteogenic medium (control), the scaffolds, and their ionic extract. We observed that ALP activity was higher in hASCs grown on the BioS-2P/F18 scaffolds than in hASCs cultured with the ionic extract or the osteogenic medium on day 14. Moreover, the dissolution product group and the control exhibited deposited calcium, which peaked on day 21. Gene expression profiles of cell cultured using the BioS-2P/F18 scaffolds and their extract were evaluated *in vitro* using the RT$^2$ Profiler polymerase chain reaction (PCR) microarray on day 21. Mineralizing tissue-associated proteins, differentiation factors, and extracellular matrix enzyme expressions were measured using quantitative PCR. The gene expression of different proteins involved in osteoblast differentiation was significantly up-regulated in hASCs grown on the scaffolds, especially BMP1, BMP2, SPP1, BMPR1B, ITGA1, ITGA2, ITGB1, SMAD1, and SMAD2, showing that both the composition and topographic features of the biomaterial could stimulate osteogenesis. This study demonstrated that gene expression of hASCs grown on the scaffold surface showed significantly increased gene expression related to hASCs cultured with the ionic extract or the osteogenic medium, evidencing that the BioS-2P/F18 scaffolds have a substantial effect on cellular behavior of hASCs.

**KEYWORDS**

Biosilicate, F18 glass, gene expression, osteogenesis, scaffold

## 1 | INTRODUCTION

Annually, approximately 15 million bone fracture cases are estimated worldwide and more than 9.0 million correspond to osteoporotic fractures.[1,2] Indeed, bone is the second tissue most often replaced, and the demand for bone tissue will certainly increase as the population grows. Hence, it is vital to establish new therapies that overcome the drawbacks of conventional grafts to improve the implantation outcomes and the quality of life of patients.[1,3,4]

The development of bone tissue engineering (BTE) represents a promising approach with great potential for repairing bone defects. Scaffolds play an essential role in BTE since these three-dimensional structures facilitate the maintenance, restoration, or enhancement of the function of the injured organ.[5,6] The ideal scaffold for BTE should function as a template for three-dimensional tissue growth, providing an interconnected macroporous network with an appropriate pore size distribution that promotes vascularization, nutrient delivery, and discharge of metabolic waste. Moreover, the scaffold must be

  

degradable, nontoxic to cells, resorbed at the same rate as tissue regeneration, and must be strong enough to avoid the breakdown of the porous structure.[4-6]

Some of the most promising biomaterials for application in BTE are the bioactive glasses. Bioglasses have been widely studied as bone grafts because they stimulate the formation, precipitation, and deposition of calcium phosphates enhancing osseointegration; moreover, depending on composition, they can be osteoinductive. Among these biomaterials, the specific composition $23.75Na_2O$–$23.75CaO$–$48.5SiO_2$–$4P_2O_5$ (wt.%) is known as Biosilicate® glass–ceramic. This bioactive glass–ceramic, baptized as BioS-2P, has some relevant properties such as osteoconductivity, osteoinductivity, and bactericidal action; furthermore, it is noncytotoxic and nongenotoxic.[7] When BioS-2P is in contact with simulated body fluid (SBF), they form a hydroxycarbonate apatite (HCA) layer in approximately 6 hr.[8] Also, the reactions on the BioS-2P surface release $Si^{4+}$, $Ca^{2+}$, $Na^+$, and $PO_4^{3-}$ ions that stimulate gene expression of different factors that are deeply involved in the differentiation and proliferation of osteoblasts, promoting rapid bone formation.[9-11] In a previous study, Ferraz et al. analyzed the expression of 23.794 genes related to osteogenic differentiation of mesenchymal stem cells (MSCs) grown on BioS-2P and Bioglass®45S5. BioS-2P significantly up-regulated 5 genes and down-regulated 3 genes compared with 45S5. In the same way, BioS-2P significantly up-regulated 15 genes and down-regulated 11 genes compared with polystyrene (control), whereas 45S5 significantly up-regulated 25 genes and down-regulated 21 genes compared with control. This showed the remarkable osteostimulation property of these biomaterials.[11] Despite all these properties, the Biosilicate scaffolds have low compressive strength (<0.1 MPa), which makes their clinical application difficult. For this reason, a novel approach was used to produce high-strength scaffolds, which consists of recoating the Biosilicate scaffolds with F18 bioglass. F18 bioactive glass ($SiO_2$–$Na_2O$–$K_2O$–$CaO$–$MgO$–$P_2O_5$ system) was chosen because it flows without crystallizing at temperatures above 600°C, bridging the micro-gaps in the Bioglass®-struts without clogging the pores. Moreover, F18 has remarkable bioactivity and a very strong antimicrobial activity.[12-14]

The aim of this study was to evaluate the gene expression profile of the human adipose-derived stem cells (hASCs) grown on the Biosilicate® (BioS-2P)/F18 bioactive glass and cultured with their dissolution products. BioS-2P/F18 scaffolds and their extract were used for the first time to culture hASCs for up to 21 days. hASCs are an interesting source of cells for BTE since they are easily harvested in high quantity and they have high potential to differentiate in osteoblasts.[15] Initially, cell viability was verified using a fluorescence method. Then, both bone formation and calcium content were assayed by Alizarin Red S (ARS). And ALP formation was visualized using a staining method and confirmed by alkaline phosphatase (ALP) activity. We also investigated by PCR array the gene expression of osteoblasts grown on the BioS-2P/F18 scaffolds related to their ionic dissolution or the control.

## 2 | MATERIALS AND METHODS

### 2.1 | Materials

Fully reticulated polyurethane foam with 45 ppi (pores per inch) donated by Recticel (Belgium) was used as a sacrificial template for the replication method. The foam was supplied in 30 mm thick sheets, which were cut into $30 \times 15 \times 15$ mm$^3$ pieces. For the preparation of the Biosilicate glass–ceramic precursor, we used $Na_2CO_3$ (Vetec), $CaCO_3$ (PA–JT Baker), $SiO_2$ (Zetasil2–Santa RosaMining Co.), and $Na_2HPO_4$ (PA–JT Baker). The powder mixture was melted in a Pt crucible for 1 hr at 1350°C and then quenched by splat cooling. This process was carried out 3 times to obtain a homogeneous glass. Finally, the melt was poured into water to obtain glass frits with a size of less than 5 mm. The glass frit was heat-treated at 750°C/6 hr. After this, the glass–ceramic frit (BioS-2P) was ball-milled to particle size of 5 μm. F18 bioactive glass (average particle size ~5 μm) powder was kindly provided by Vetra High-Tech Bioceramics.

### 2.2 | Scaffold fabrication

Polymer sponge replication was used to produce the reticulated glass–ceramic foam-like scaffolds. A suspension was prepared using Biosilicate (BioS-2P) powder (30 v/v%), ethyl alcohol (66 v/v%), and polyvinyl butyral (PVB) as the binder (4 v/v%). The 45 ppi (pores per inch) polyurethane foam template (Recticel–Belgium) was immersed in the slurry, took out, and squeezed to remove the excess slurry. The samples were dried at room temperature for at least 12 hr, sintered at 900°C for 3 hr, and cooled down to room temperature. Then, to increase the mechanical strength of the BioS-2P scaffolds, they were immersed in a 15% (v/v) F18 glass based-suspension and again sintered at 800°C for 3 hr to obtain the BioS-2P/F18 scaffolds.

### 2.3 | Cell culture

Human adipose-derived mesenchymal stem cells (hASCs) were purchased from Sciencell and maintained in a nitrogen atmosphere in a Locator™ Plus Rack and Box System (Thermo Scientific). All cell culture experiments were carried out in a biological safety cabinet (Microzone Corporation–model BK-2-4) under sterilized conditions.

At 2–4 passage, hASCs were cultured in 24-well polystyrene plates (Cellstar®-Greiner) using mesenchymal stem cell medium (MSCM) (Sciencell–Canada) in a humidified incubator (Thermo Scientific–Steri-Cycle) for 4 days at 37°C with 5% $CO_2$ until confluent. The medium was changed every 2 days. To differentiate these cells into mature osteoblastic cells, hASCs were seeded in mesenchymal stem cell osteogenic differentiation medium (MODM) (Sciencell–Canada) at a density of $1 \times 10^5$ cells.cm$^{-2}$. MODM was changed every 3–4 days for 7, 14, or 21 days relying on the tests. The samples treated in this way were used as the control (polystyrene). Also, hASCs were cultured on the BioS-2P/F18 scaffolds. The scaffolds were previously sterilized in a convection oven

(Thermo Scientific–model 6,520) at 180°C for 3 hr. Then, the scaffolds were immersed for 1 hr in vitronectin solution, and hASCs were passaged on the scaffold at a density of $1 \times 10^5$ cells.cm$^{-2}$ following the same procedure used for the control. Additionally, the ions of the scaffolds were extracted in MODM as follows, 10 ml of MODM was left with 1 g of the scaffold for 48 hr in humidified incubator at 37°C with 5% $CO_2$, filtered with a sterilized syringe filter (VWR–Ø 0.2 μm), and MODM was added to reach a final volume of 50 ml. This dissolution product was used to differentiate the hASCs following the same procedure used for the control.

The concentration of calcium ions was determined by a photometric method, the concentration of phosphate groups was determined using a UV photometric method, and the concentration of sodium ions was established by an ion-selective electrode at the Maricondi Laboratory (São Carlos–Brazil).

## 2.4 | Evaluation of cell viability

Live/dead staining was performed for the control and the experimental samples (the dissolution product group and the scaffolds). The staining solution was prepared by mixing 2 μl Calcein AM (Invitrogen–Life Technologies) and 4 μl ethidium homodimer-1 (Invitrogen–Life Technologies) in 2 ml of PBS. The osteogenic medium was removed on day 2 and staining solution was added to the dissolution product group (0.5 ml), the control (0.5 ml), and the scaffold group (1 ml), then all samples were incubated for 30 min at room temperature. Cells were observed using a microscope with a fluorescence light source (Lumen Dynamics–X-Cite series 120Q). Calcein AM (488 nm) and EthD-1 (543 nm) were excited using an optical filter.

## 2.5 | Alkaline phosphatase staining

Cells were stained for the control and the experimental samples using SIGMA FAST™ BCIP/NBT (5-Bromo-4-chloro-3-indolyl phosphate/Nitro blue tetrazolium) tablets (Sigma–Aldrich). One tablet, dissolved in 10 ml of water, provides 10 ml of ready-to-use buffered substrate solution, which contains BCIP (0.15 mg/ml), NBT (0.30 mg/ml), Tris-buffer (100 mM), and $MgCl_2$ (5 mM), pH 9.25–9.75. The osteogenic medium was removed at 7, 14, and 21 days and the cells were rinsed twice with 0.17 M TRIS-buffer (pH 7.3, 37°C). 1 ml of BCIP/NBT (Sigma–Aldrich) was added to each well, and the preparation was incubated for 10 min at room temperature. The BCIP/NBT solution was removed, and the cells were rinsed with deionized water. ALP-positive cells were stained blue.

## 2.6 | Alkaline phosphatase activity

For the assessment of the alkaline phosphatase (ALP) activity, the cells were cultured for 7, 14, and 21 days. ALP activity was measured using an ALP Colorimetric Assay Kit (Abcam–Canada) according to the manufacturer's procedure. This method uses *p*-nitrophenyl phosphate (pNPP) as a phosphatase substrate that, in the presence of ALP, is dephosphorylated, producing yellowish *p*-nitrophenol ($OD_{max}$ = 405 nm). Cells were washed with cold PBS (Gibco) and resuspended in 50 μl of assay buffer. Then, they were homogenized using a Dounce homogenizer and centrifuged at 4°C at 1000 rpm for 15 min. 5 μl of this lysate was added to a 96-well plate with 75 μl assay buffer and 50 μl *p*NPP. The samples were covered to protect them from light for 1 hr at 25°C. Then, 20 μl stop solution (NaOH) was added to the wells, and the outputs were measured at O.D. 405 nm on a microplate reader (Tecan). Enzymatic activity was normalized to DNA content measured with the NanoVue Plus spectrophotometer (GE Healthcare). ALP activity was expressed as μmol. min$^{-1}$.ml$^{-1}$.μg$^{-1}$ DNA. To compare with the 3D scaffolds, we measured ALP activity for a dense specimen of Biosilicate, that is, without the porous scaffold structure.

## 2.7 | Alizarin red S (ARS) staining quantification

Mineralization was evaluated quantitatively and qualitatively using Alizarin Red S (Sigma) after 7, 14, and 21 days of hASCs culture in osteogenic medium. The medium and the scaffolds were removed from the wells, and the cells were washed with phosphate-buffered saline (1xPBS) 3 times and fixed in 4% formaldehyde for 15 min at room temperature. These cells were then washed 3 times (5–10 min each) with distilled water. The fixed samples were stained with 40 mM ARS and incubated at room temperature for 30 min with gentle shaking. The cells were washed 5 times with distilled water, and the plate was inspected using a microscope, and images were taken. After this qualitative test, the plate was stored at −20°C prior to dye extraction. The stained nodules were then incubated in 10% acetic acid (Caledon) and incubated for an extra 30 min with shaking at room temperature. The collected cells were heated to 85°C for 10 min and centrifuged at 20,000xg for 15 min. The supernatant was neutralized with 10% ammonium hydroxide (Sigma) and the absorbance was determined at 405 nm. The level of ARS staining in the samples (mol/L) was determined according to a linear regression equation derived from a standard curve of known ARS concentrations.

The SPSS 25.0 (IBM) software was used for statistical analysis of ALP activity and calcium content. All data were represented as mean ± S.D., and validated by *t* test if complied with the normal distribution and if not by the nonparametric Wilcoxon Rank-Sum test. Statistical significance was set at $p < 0.05$. The experiments were repeated in triplicate for each treatment group.

## 2.8 | RNA extraction and RT$^2$ gene profiler PCR array

hASCs were cultured in 24-well plates following the same procedure as in Section 2.3. After 21 days of culture in the osteogenic medium, the cells were washed once with PBS and harvested for total RNA extraction with the RNAeasy Minikit (Qiagen–Canada) according to

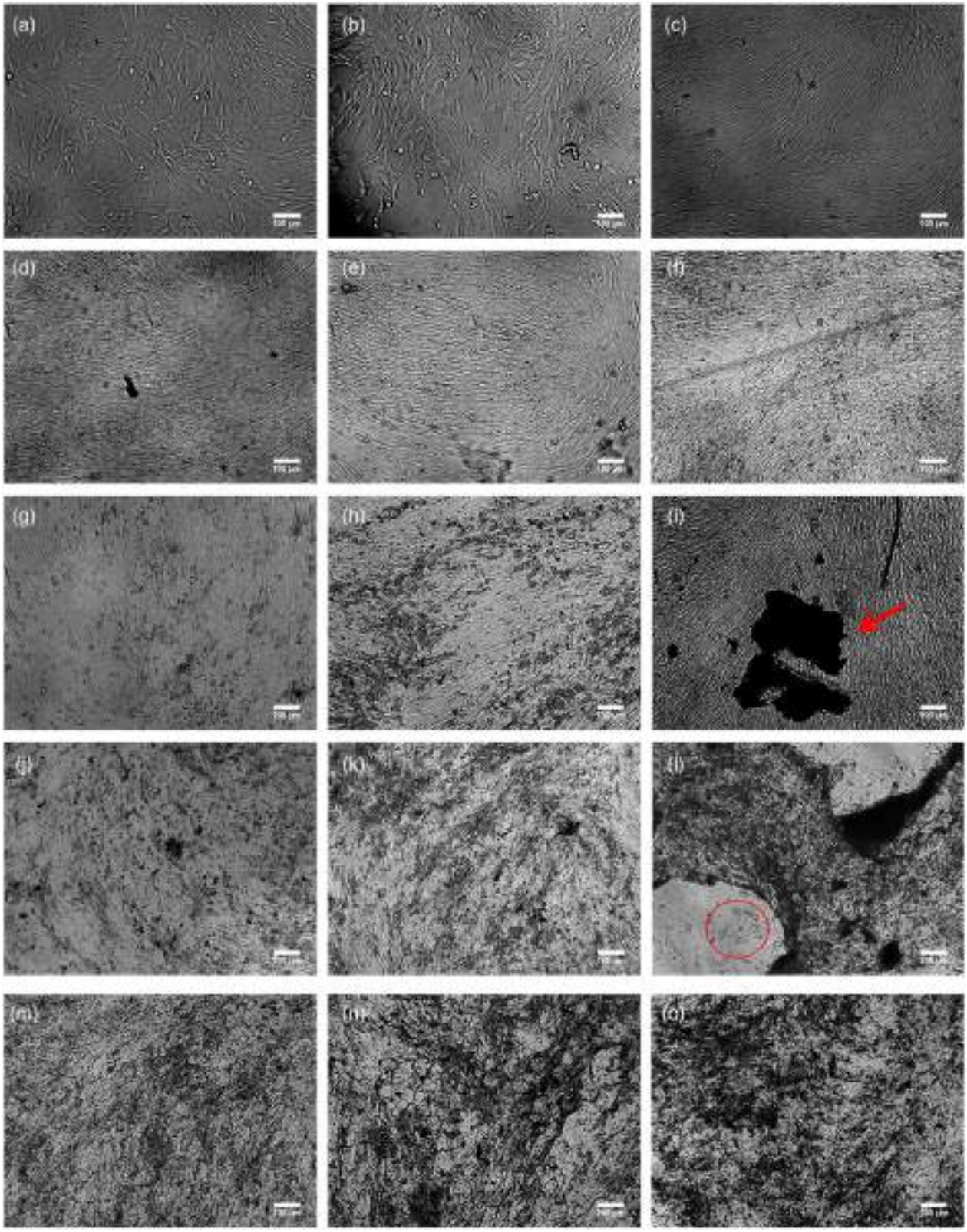


**FIGURE 1** Cell morphology of hASCs (M ×100) at passage 2. (a) in MSCM (control) after 1 day, (b) passaged on the scaffold using MSCM after 1 day, and (c) in MSCM after 4 days. Cell morphology of hASCs (M ×100) after 3 days in osteogenic medium (MODM) for (d) the control, (e) the dissolution product group, and (f) the scaffolds; after 7 in MODM for (g) the control, (h) the dissolution product group, and (i) the scaffolds (the red arrow points the particles released by the scaffold); after 14 days in MODM for (j) the control, (k) the dissolution product group, and (l) the scaffolds (the red circle is over a place with little confluence); after 21 days in MODM for (m) the control, (n) the dissolution product group, and (o) the scaffolds. Scale bar represents 100 μm

the manufacturer's protocol. Total RNA was then converted to cDNA by the proprietary first-strand cDNA synthesis kit included in the PCR array system (Qiagen–Canada). The osteogenic pathway PCR array system (Cat#: PAHS-026Z, Qiagen–Canada) was selected for this study. The cDNA and SYBR Green Master Mix were added to each well of the array plate according to the manufacturer's instruction. Real-time PCR was performed on the Steponeplus™ Real-Time PCR system (Thermo Fisher Scientific). All target gene expression results were normalized to ACTB, RPLP0, GAPDH, and HPRT1. Statistical analysis and fold change calculations were performed with the provided software at the Qiagen PCR Array Data Analysis web portal (https://geneglobe.qiagen.com/ca/analyze/). Gene expression changes of target genes were compared with the control group using the student *t* test, and values of $p < 0.05$ were considered to be statistically significant. The experiments were repeated in triplicate for each treatment group.

## 3 | RESULTS AND DISCUSSION

### 3.1 | Morphological characteristics of hASCs

hASCs (passage 2) cultured with MSCM (Figure 1a) or with the BioS-2P/F18 scaffolds (Figure 1b) showed similar cell morphology with characteristic elongated spindle shape, monolayer appearance, and cell size. This indicates that the scaffolds are not generating any adverse environment for cellular growth during expansion. Figure 1c shows that hASCs cultured in MSCM for 4 days reached around 100% confluent. Cells presented both hASCs morphology and healthy state, being appropriate for passaging and differentiating *in vitro* using MODM.

As can be observed in Figure 1(d,e,f), the cells showed good confluence after 3 days in osteogenic medium and, in general, the morphology of the experimental samples and the control are similar. After 7 days of incubation with osteogenic differentiation medium, dark brown cell multilayers were observed under the microscope (Figures 1g-l). This phenotypic change is attributed to matrix maturation. After matrix secretion by the osteoblasts, the maturation phase is performed, generating polymerization of collagen into an array of fibrils, binding of calcium to collagen fibrils, and formation of protein-glycosaminoglycan complexes.[16] At 14 days, it is noted that the dark zone increased in the plates. During this stage known as mineralization, calcium and phosphate precipitation takes place, followed by deposition of hydroxyapatite [$Ca_{10}(PO_4)_6(OH)_2$] crystals within the organic bone matrix (Figure 2). Mineralization was considerably higher for the scaffolds and the dissolution product group than for the control (Figures 1j-l). This showed that both the scaffolds and their extract stimulated mineralization.

The scaffolds presented zones where the confluence decreased markedly (Figure 1l). This effect was caused by the particles released (Figure1i) for the material into the media, which accumulated on the cells, disrupting the homeostasis and causing cell death. In cells, proliferation and differentiation are regulated by external signals that involve the activation of complex mechanisms of intercellular communication. In humans, these mechanisms are based on cells communicating with each other by noncontacted endocrine, autocrine, or paracrine signaling via secreted chemicals, and cell-contact-dependent signaling. Several studies have shown that cell–cell interactions that happen by contacting among neighboring cells, transferring of intracellular proteins, or soluble paracrine factors play a critical role in preserving stem cell homeostasis in culture.[17,18]

Moreover, cellular interaction with extracellular matrix (ECM) and neighboring cells is necessary for osteoblast survival, proliferation, and differentiation.[18] These factors could have been altered by the released particles in the cultures, affecting the confluence on the bottom of the wells for the scaffold samples. Nevertheless, the confluence for this group was more than 85% being enough to get healthy osteoblast cultures. Figure 1(m,n,o) showed a considerable increment in the nodule formation, mainly in the scaffolds and the dissolution product group on day 21.

### 3.2 | Assessment of cell viability

Live/dead tests were done for the samples and the control to evaluate the cell viability of hASCs cultured in MODM for 2 day. The green spindle-shaped cells were live cells. As can be seen in Figure 3(a,b,c), almost all cells were alive at the bottom of the wells for the control, the scaffolds, and the dissolution product group and a negligible amount of dead cells was found for all conditions. In brief, the material did not generate a toxic environment for the cell differentiation, which allowed cell growth and osteogenesis to perform normally. These results suggest that hASCs were able to adhere and proliferate on the material surface. As is known, surface properties, such as, topography, chemistry, or surface energy establish how biomolecules adhere to the biomaterial surface; moreover, topography can help to induce the expression of specific factors involved in osteogenesis.[19,20] Hakki et al. found that the attachment and the expression of key factors, such as, BSP (bone sialoprotein), BGLAP, SPP1, ALP, COL I, MMP2, MMP9, different collagen types, FGFs, BMP2, BMP3, BMP5, BMP6, and their receptor increased on roughness surfaces of titanium implants.[20] When the implant is in contact with the cells, the attachment and the diffusion of the active matrix over porous roughness facilitate early osseointegration.[20]

The first contact between hASCs and material surface created focal adhesions that were mediated by vitronectin; this glycoprotein possesses the arginine-glycine-aspartic acid (RGD) sequence, which is recognized for the cell surface receptors, such as, integrins. When integrins bind to vitronectin, specialized protein clusters are formed, inducing both adhesion and directed assembly of actin filaments and signaling components, as well as cytoskeletal tension changes generating a series of mechanochemical signal pathways; this interaction between cells and material performs a crucial role in osteoblast survival, proliferation, and differentiation that induce osteogenesis process.[18,21] Therefore, the BioS-2P/F18 scaffolds fostered cell adhesion

during the initial stage of osteogenesis, which is essential to define the fate of the cells. Also, the ions in the media induced genetic control over the genes that regulate osteogenesis.[5]

### 3.3 | ALP activity

ALP is an early marker of osteogenic differentiation involved in the formation of bone-like nodules that are employed during matrix mineralization.[22] This metalloenzyme catalyzes the hydrolysis of phosphate esters, generating the phosphate groups that are necessary for the formation and deposition of the hydroxyapatite during the osteogenic process. In its active site is produced serine phosphate, which is able to react with water at basic pH producing inorganic phosphate.[23] Moreover, ALP fosters mineralization by hydrolyzing extracellular inorganic pyrophosphate, which is an inhibitor of mineralization.[24]

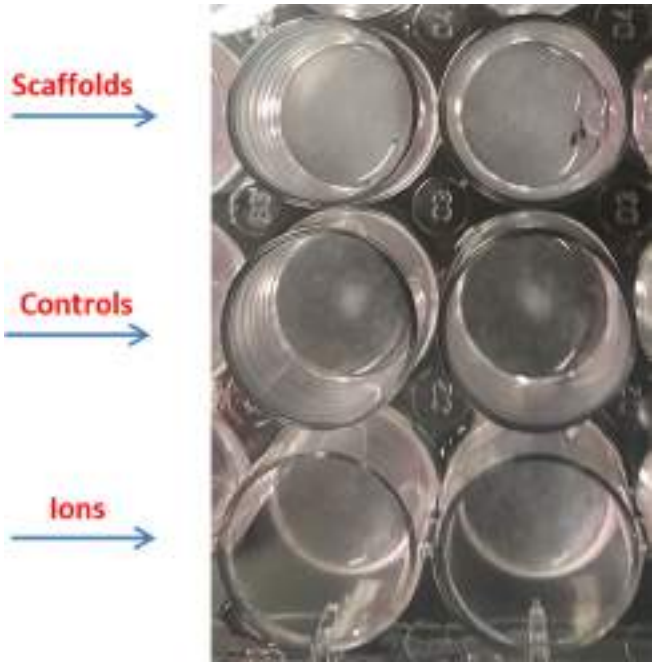


**FIGURE 2** Photo of hASCs cultured in 24–well plate using osteogenic medium for 14 days

ALP was assayed qualitatively and quantitatively; ALP staining was done for the dissolution product group, the control, and the scaffolds on 7, 14, and 21 days. As can be seen in Figure 4, all groups displayed positive ALP activity on days 7 and 14. They presented a dark purple color that was generated by the formation of the insoluble NBT diformazan because of the catalytic activity of ALP.[25] On the other hand, all groups showed a light blue color at day 21 since the ALP concentration diminished after 14 days. As is known, ALP is expressed early in the osteoblastic lineage concomitantly with osteoid production; however, as matrix mineralization occurs, other genes, such as, osteocalcin begin being up-regulated and ALP starts to be down-regulated.[23,26]

ALP activity was confirmed for all groups. All samples showed an increase in ALP activity from 7 to 14 days (Figure 5). At day 7, the control showed significantly higher ALP activity compared with those of the BioS-2P (dense specimen) and the BioS-2P/F18 scaffolds and the dissolution product group. When the scaffolds are in contact with the medium, these begin releasing particles that can alter homeostasis (Figure 1I); and during an early stage of culture, the cells were adapting to these conditions, which could have affected the ALP production. A similar behavior was observed for the dissolution product group, whose medium could have suffered ionic saturation affecting ALP activity up to day 7, reaching normal cellular activity in 2 weeks. On day 14, the BioS-2P/F18 scaffolds led to a significantly higher value of ALP compared with the control because these kinds of biomaterials help in osteogenesis process not only for the high bioactivity of Biosilicate and F18 glass, but also for the surface properties of the material that can induce factors that regulate osteoblastic differentiation. Moreover, their highly interconnected porous structure mimics the morphology of trabecular bone, creating an appropriate environment for hASCs migration, cellular growth, and differentiation. The dissolution product group and the BioS-2P scaffolds induced significantly higher values of ALP activity than the control at day 14, confirming that chemical and surface properties of materials stimulate

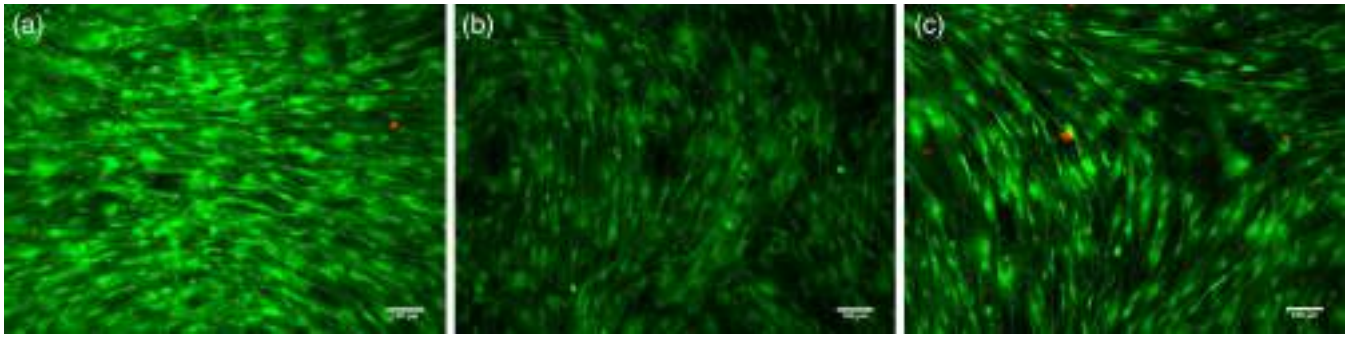


**FIGURE 3** Photos of the live/dead tests taken with an optical microscope. hASCs were cultured in MODM for 2 days: (a) the control, (b) the dissolution product group, and (c) the scaffold samples. All images are from bottom of the wells. Green parts represent live cells, and red dots represent dead cells. Scale bar represents 100 μm. The images of the live and dead cells were merged using the ImageJ software

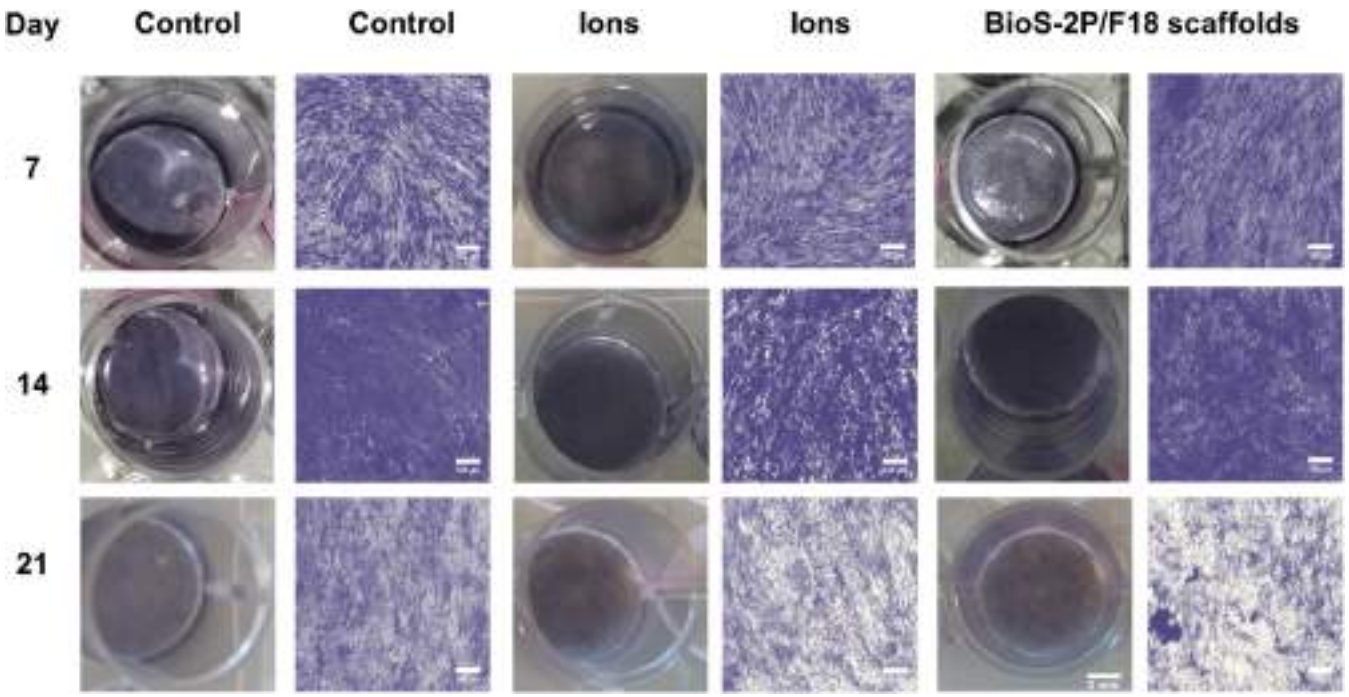


**FIGURE 4** hASCs cultured with MODM for 7, 14, and 21 days were stained with BCIP-NBT. The scale bars of photos taken with the optical microscope are equal to 150 μm, and the one of photo from the well represents 3 mm

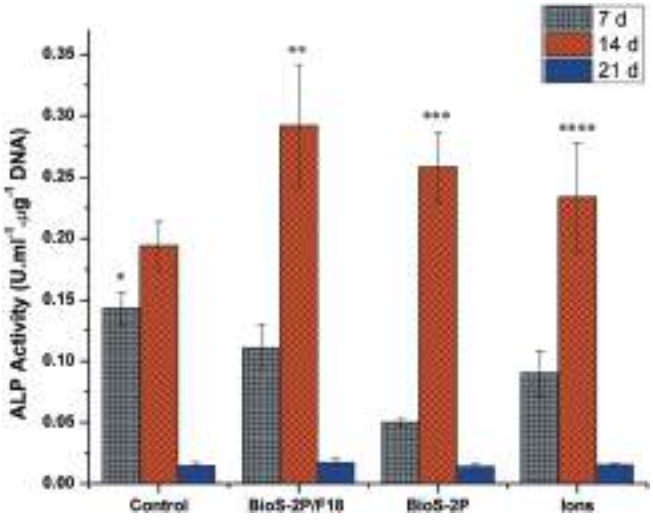


**FIGURE 5** ALP activity (μmol.min$^{-1}$.ml$^{-1}$.μg$^{-1}$ DNA) for hASCs cultured with MODM (control), dissolution product group (ions), and the BioS/2P and BioS-2P/F18 scaffolds at 7, 14, and 21 days, normalized with DNA content. *$p$ < 0.05 versus BioS-2P/F18. *$p$ < 0.05 versus BioS-2P. *$p$ < 0.05 versus ions. **$p$ < 0.05 versus control. **$p$ < 0.05 versus BioS-2P. **$p$ < 0.05 versus ions. ***$p$ < 0.05 versus control. ****$p$ < 0.05 versus control

osteogenesis. Nevertheless, interconnected porous structure induced a stronger effect since it imitates ECM.

Due to the large surface area, the scaffolds released a high amount of ions that can induce the osteogenic expression. Among them, Si ions can induce osteogenic differentiation in human bone marrow stromal cells activating osteogenic-related signaling pathways that elevate ALP activity and the expression of factors, such as, osteocalcin (BGLAP), runt-related transcription factor 2 (RUNX2), collagen type I (COL1), and osteopontin (SPP1).[27,28] Other ions released for this biomaterial are phosphate, $Na^+$, and $Ca^{2+}$ that are necessary for hydroxyapatite formation and foster the expression of some osteoblastic genes.[5,7,8,29] On day 21, ALP activities for the samples and the control were down-regulated, which is confirmed for ALP staining that produced a pale color in all tests because of a little amount of ALP presented in all groups. In different studies, ALP activity has shown an increase in the first 14 days and a substantial decrease in the third week.[30,31] Shu et al. found that ALP activity of the nano-doped calcium phosphate cement delivery system of GLI family zinc finger 1 (IGF1) and bone morphogenetic protein 2 (BMP2) increased during 12 days.[31] Mahdavi et al. found that ALP expression of the equine adipose-derived stem cells (eASCs) grown on nano-bioactive glass-coated poly(l-lactic acid) nanofibers scaffold incremented in the first 2 weeks. The enzymatic activity increased when the scaffold was coated with nano-bioactive glass, peaking after 14 days and down-regulating at 21 days.[30] Yu et al. found that Ti-6Al-4 V with zinc-modified calcium silicate coatings up-regulated the bone marrow-derived pericytes for 2 weeks, reaching ALP peak at 14 days and a decrease at day 21.[27]

### 3.4 | Alizarin red staining and quantification

hASCs were stained with ARS on days 7, 14, and 21. This permitted evaluating the formation of red nodule visually in all groups. As can be seen in

Figure 6a, deposited calcium increased from 7 to 21 days. Subsequently, the deposited calcium content was quantified on days 7, 14, and 21.

This assay is not appropriate to quantify calcium for hASCs grown on the BioS-2P/F18 scaffolds because Biosilicate and F18 glass contain calcium, which is released into the medium and accumulates at the bottom of the wells increasing the quantity of calcium detected. Figure 6b shows that both groups presented similar calcium content at 7 and 14 days. On day 21, the dissolution product group induced a significantly higher amount of calcium than the control, this increment was induced by ions released for the scaffolds, which stimulated osteogenesis. Similar results have been found in others studies with MSCs; after quantification of the deposited calcium content during 3 weeks of osteogenic induction, the calcium nodule formation increased as time went by, peaking at day 21.[32,33] There are different factors that can lead to a better mineralization process, such as, the composition. Bageshlooyafshar et al. observed that Zn silicate mineral nanoparticles increased mineralization of eASCs, and Yang et al. found that silica nanoparticles were able to increase mineralization, proliferation, and differentiation of hMSCs at day 21.[22,33]

## 3.5 | Gene expression

Table 1 shows the ion concentrations of the osteogenic medium used to differentiate the hASCs.

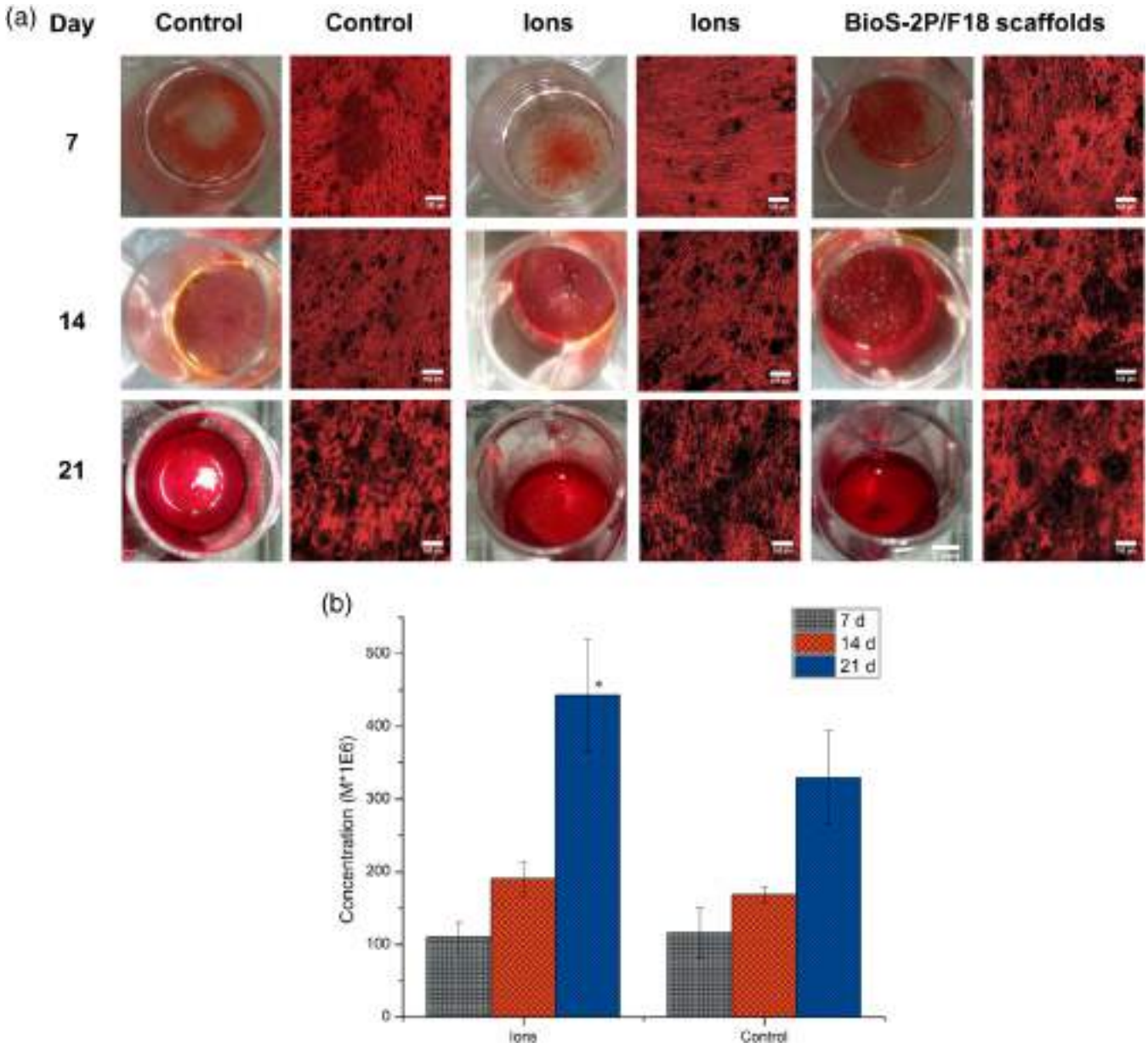


**FIGURE 6** Mineralization of hASCs evaluated by Alizarin Red S. (a) Photos of hASCs stained with ARS after 7, 14, and 21 days using MODM (control), the dissolution products (ions), and the BioS-2P/F18 scaffolds. (b) Quantification of calcium deposited for the dissolution product group and the control using ARS on days 7, 14, and 21. *$p < 0.05$ versus control

**TABLE 1** Concentration of calcium, sodium, and phosphate ions released by the BioS-2P/F18 scaffolds after being in contact with the osteogenic media for 48 hr at 37°C

| Ions | Concentration mg.L$^{-1}$ |
|---|---|
| Calcium | 14 |
| Phosphate | 25 |
| Sodium | 138 |

In this work, we tested the expression of 84 genes related to osteogenesis in its different stages, proliferation, matrix maturation, and mineralization. Among these genes, we only reported genes that exhibited at least reasonably detected gene expression. These factors are recognized to have essential roles during osteogenesis and are vital in the mineralization process.[34,35]

For the dissolution product group, among the 67 genes that were expressed, 22 were up-regulated, 25 were down-regulated, and 20 showed no change with respect to gene expression of the control (Table 2). Among these, 6 were significantly up-regulated, and 5 were significantly down-regulated. For the scaffold group, among the 70 genes that were expressed, 32 genes were up-regulated, 28 were down-regulated, and 10 showed no change with respect to gene expression of the control (Table 2). Among these, 12 were significantly up-regulated, and 8 were significantly down-regulated. Also, the scaffolds (63 genes expressed) induced up-regulation of 22 genes and down-regulation of 18 genes compared with the dissolution product group (Table 3). Among these, 3 were significantly up-regulated, and 2 were significantly down-regulated. Table 4 shows the ratios of down- and up-regulated genes per gene groups for the scaffold group versus the control, the dissolution product group versus the control, and the scaffold group versus the dissolution product group. Green represents relative higher expression and red represents the opposite. In general, the data reflected that more genes were up-regulated per group for the scaffolds relative to the control than for the dissolution product group versus the control, and the scaffolds versus the dissolution product group at 21 days (Table 4). hASCs grown on the scaffold surface showed higher gene expression compared with cells cultured with the ionic extract or the osteogenic medium because the BioS-2P/F18 scaffolds are highly porous with interconnected pore networks that facilitate nutrient and oxygen diffusion as well as waste removal, being able to support cell colonization, proliferation, and differentiation of hASCs. This structure can mimic the *in vivo* bone environment stimulating the cellular differentiation to generate new bone tissue.[36] Moreover, F18 glass and Biosilicate are mainly composed of calcium, phosphorus, and silicon ions that have proven to boost the osteogenic process.

The ionic products of silicate-based glasses foster gene transcription in osteoblasts because of the activation of several genes of the osteogenic cells.[5,37] $Ca^{2+}$ ions have a vital role in mineralization, activate the expression of factors that control the human osteoblast proliferation (insulin-like growth factor 1/2 [IGFI/II]), and stimulate osteoblast differentiation. Inorganic phosphates regulate mineralization, and Si promotes the osteoblast differentiation.[5,37] In addition, hydrophilic surfaces increase cell adhesion aiding in cell spreading over the biomaterial, whereas the geometric microenvironment of the scaffold can influence the cellular behavior.[38-40]

As can be seen in Table 2, RUNX2 was up-regulated for the dissolution product group and the scaffolds; no significance differences were observed among all treatment groups. RUNX2 is considered the most important factor of the intramembranous ossification, which is the mechanism that leads to osteogenesis when MSCs are cultured *in vitro* using an osteogenic medium. This factor is targeted in most of the pathways involved in osteogenesis, activating some genes that are essential for this process, such as, osteopontin and bone sialoprotein.[41,42] BMP2 is its major regulator, and during BMP pathway, the complex SMAD-1/5/8 (SMAD family member 1/5/8) forms a heterotrimeric transcription complex with SMAD family member 4 (SMAD4), which travels to the nucleus where it can interact with different factors, such as, RUNX2 to initiate different processes that encourage bone formation.[43] Some studies have found that RUNX2 exhibits a gradual increment during the osteogenic process since this factor is a positive transcriptional regulator of genes, such as, collagen type I alpha 1 (COL1A1), ALP, and BGLAP, which are vital for the matrix maturation and mineralization; moreover, RUNX2 is considered the key transcriptional factor to initiate bone formation.[36,41] ALP, other key osteogenesis gene, was down-regulated in all groups, which fits well with the results of ALP activity (Figure 5).

Different relevant proteins for osteoblast differentiation were up-regulated in hASCs grown on the scaffold surface and in hASCs cultured with the dissolution products, especially, BMP1, BMP4, BMP5, BMPR1A, BMPR1B, BMPR2, SMAD1, SMAD2, and SMAD4. hASCs grown on the scaffolds induced significant up-regulation of BMP1 (Tables 2 and 3). These points that the scaffolds were beneficial for matrix development and osteoblast differentiation. This enzyme is responsible for the cleavage of the C-terminal procollagen propeptides of the major fibrillar collagen types I–III necessary for the development of the ECM; moreover, BMP1 induces cartilage and bone formation.[34] Additionally, hASCs grown on the scaffolds induced significantly stronger up-regulation of BMP2 than hASCs cultured with the dissolution products related to the control, which was caused by the topographic feature of the scaffolds. Castro-Raucci et al. demonstrated that modifications in the material topography affect osteoblast differentiation of the human mesenchymal stromal cells by acting on several mechanisms, including modulation of the signaling pathways of distinct growth factors, such as, BMPs. The modified surface may up-regulate the endogenous expression of BMP2 in osteoblastic cells, increasing the osteogenic potential.[44] BMP2 is part of the major group of bone morphogenetic factors that modulates diverse mesodermal developmental processes and intervenes in many processes involved in angiogenesis; moreover, BMP2 has shown to be the most osteogenic bone morphogenetic protein, being able to foster bone formation around implants.[45] Also, it helps in the regulation of postnatal development of mesenchymal skeletal tissues and skeletal repair.[45,46] Mareddy et al. found that BMP2 treatment leads to better bone nodule formation and calcium deposition and, together with fibroblast growth factor 2 (FGF2), facilitates osteogenesis *in vivo* and

**TABLE 2** $RT^2$ PCR array gene profiler results for hASCs grown on the scaffolds relative to the control, and for hASCs cultured with the dissolution products relative to the control. Fold regulation values greater than 2 are up-regulated, fold regulation values less than 2 are down-regulated, and fold regulation values between 2 and −2 indicate no change. *Measure with *p*-value <0.05 is considered statistically significant. Dash (–) means that the relative expression level is low in both the control and the test samples

| Symbol | Fold regulation ion dissolution | Fold regulation scaffolds |
|---|---|---|
| Bone matrix proteins | | |
| ALP | −2.67 | −97.98* |
| BGLAP | −282.82 | −178.10 |
| BGN | — | 4.43 |
| SPP1 | 1.25 | 13.29* |
| Bone morphogenetic protein (BMP) superfamily | | |
| BMP1 | −1.95 | 28.62* |
| BMP2 | 80.87* | 125.26* |
| BMP3 | −1.18 | — |
| BMP4 | — | 42.50 |
| BMP5 | 33.82 | 11.55 |
| BMP6 | — | 1.68 |
| BMP7 | 1.42 | 4.65 |
| GDF10 | 7.28* | — |
| TGFB1 | 1.78 | 5.67 |
| TGFB2 | −20.41* | −26.84* |
| TGFB3 | 36.74 | 6.65 |
| BMP receptors | | |
| BMPR1A | 5.78 | −1.23 |
| BMPR1B | — | 51.28* |
| BMPR2 | 4.46 | 1.52 |
| Receptors | | |
| ACVR1 | −78.84 | −12.20 |
| CALCR | −187.51* | −256.34* |
| EGFR | −1.98 | — |
| FGFR1 | −2.76 | −2.26 |
| FGFR2 | −1.33 | −2.00 |
| ICAM1 | −1.14 | −3.82 |
| PHEX | −3.23 | −4.96 |
| TGFBR1 | 2.07 | −2.12 |
| TGFBR2 | −1.42 | 4.01* |
| VCAM1 | — | 23.18* |
| VDR | — | 2.06 |
| Growth factors | | |
| EGF | −9.53 | −18.40* |
| FGF1 | −1.23 | — |
| FGF2 | 124.84* | — |
| IGF2 | −33.50* | −9.44* |
| PDGFA | 1.37 | −2.42 |
| VEGFA | 1.03 | −1.58 |
| VEGFB | −104.91* | −258.41* |
| CSF1 | — | −2.41 |
| CSF2 | −5.43 | 1.30 |
| CSF3 | −3.20 | −11.90 |

**TABLE 2** (Continued)

| Symbol | Fold regulation ion dissolution | Fold regulation scaffolds |
|---|---|---|
| Integrin receptors | | |
| ITGA1 | 5.13 | 11.32* |
| ITGA2 | 51.43 | 34.90* |
| ITGA3 | −2.88 | −3.94 |
| ITGAM | −1.18 | 33.08 |
| ITGB1 | 63.74 | 77.75* |
| Collagen | | |
| COL10A1 | 1.01 | −18.70 |
| COL14A1 | −1.78 | −101.89 |
| COL15A1 | 18.51 | — |
| COL1A1 | −1.57 | 1.09 |
| COL1A2 | 23.17 | 76.78 |
| COL3A1 | −4.38 | 2.20 |
| COL5A1 | 5.04 | 7.43 |
| Cartilage-related genes | | |
| COMP | 2.70* | 3.65 |
| SOX9 | −2.25 | 2.98 |
| Metalloproteinases | | |
| MMP10 | 29.89 | 34.97 |
| MMP2 | 9.34 | 3.65 |
| MMP8 | −2.60 | −1.79 |
| MMP9 | −11.63 | −14.13 |
| Transcription factors | | |
| NFKB1 | −11.93 | −6.60 |
| RUNX2 | 10.30 | 50.13 |
| SMAD1 | 25.02* | 9.45* |
| SMAD2 | 55.49* | 87.07* |
| SMAD3 | −3.19 | −3.69 |
| SMAD4 | — | 14.64 |
| SMAD5 | −4.41 | −6.93 |
| SP7 | −25.44 | −12.70 |
| TWIST1 | 30.81 | 31.30* |
| Other genes | | |
| AHSG | 17.76 | — |
| ANXA5 | −19.71* | −26.30* |
| CTSK | 32.64 | 22.72 |
| DLX5 | −45.99 | −351.83 |
| FN1 | 1.07 | 14.08 |
| GLI1 | −4.49 | 1.101 |
| IHH | −1.61 | −2.27 |
| NOG | — | −3.37* |
| SERPINH1 | −1.30 | 1.93 |
| TNF | — | 48.52 |
| TNFSF11 | −25.09 | −221.58 |

**TABLE 3** $RT^2$ PCR array gene profiler results for hASCs grown on the scaffolds relative to the dissolution product group. Fold regulation values greater than 2 are up-regulated, fold regulation values less than 2 are down-regulated, and fold regulation values between 2 and −2 indicate no change. *Measure with *p*-value <0.05 is considered statistically significant. Dash (–) means that the relative expression level is low in both groups

| Symbol | Fold regulation scaffolds |
|---|---|
| Bone matrix proteins | |
| ALP | −36.66 |
| BGLAP | – |
| BGN | 5.49 |
| SPP1 | 10.60 |
| BMP superfamily | |
| BMP1 | 55.94* |
| BMP2 | 1.55 |
| BMP3 | −12.98 |
| BMP4 | 110.28 |
| BMP5 | −2.93 |
| BMP6 | 9.04 |
| BMP7 | 3.27 |
| GDF10 | −952.16* |
| TGFB1 | 3.19 |
| TGFB2 | – |
| TGFB3 | −5.52 |
| BMP receptors | |
| BMPR1A | −7.11 |
| BMPR1B | 150.82* |
| BMPR2 | −2.94 |
| Receptors | |
| ACVR1 | – |
| CALCR | – |
| EGFR | −2.97 |
| FGFR1 | 1.22 |
| FGFR2 | −1.50 |
| ICAM1 | −3.35 |
| PHEX | – |
| TGFBR1 | −4.41 |
| TGFBR2 | 5.68* |
| VCAM1 | 13.62 |
| VDR | – |
| Growth factors | |
| EGF | −1.93 |
| FGF1 | −26.70 |
| FGF2 | −210.45* |
| IGF2 | – |
| PDGFA | – |
| VEGFA | −1.63 |
| VEGFB | – |
| CSF1 | 1.59 |
| CSF2 | 7.10 |
| CSF3 | – |
| Integrin receptors | |
| ITGA1 | 2.21 |
| ITGA2 | −1.47 |
| ITGA3 | −1.37 |
| ITGAM | 38.96 |
| ITGB1 | 1.22 |
| Collagen | |
| COL10A1 | −18.93 |
| COL14A1 | −57.11 |
| COL15A1 | −15.75 |
| COL1A1 | 1.71 |
| COL1A2 | 3.31 |
| COL3A1 | 9.63 |
| COL5A1 | 1.48 |
| Cartilage-related genes | |
| COMP | 1.35 |
| SOX9 | 6.72 |
| Metalloproteinases | |
| MMP10 | 1.17 |
| MMP2 | −2.56 |
| MMP8 | 1.45 |
| MMP9 | −1.22 |
| Transcription factors | |
| NFKB1 | 1.81 |
| RUNX2 | 4.87 |
| SMAD1 | −2.65 |
| SMAD2 | 1.57 |
| SMAD3 | −1.16 |
| SMAD4 | 9.35 |
| SMAD5 | −1.57 |
| SP7 | 2.00 |
| TWIST1 | 1.02 |
| Other genes | |
| AHSG | −5.75 |
| ANXA5 | −1.33 |
| CTSK | −1.44 |
| DLX5 | – |
| FN1 | 13.16 |
| GLI1 | 4.95 |
| IHH | – |
| NOG | – |
| SERPINH1 | 2.51 |
| TNF | 4.71 |
| TNFSF11 | – |

**TABLE 4** Ratio of down- and up-regulated genes per gene group for hASCs cultured with the scaffolds relative to the control, hASCs cultured with the scaffolds relative to dissolution product group (ions), and hASCs cultured with the dissolution product relative to the control for 21 days. Dark tones represent up-regulation (green) or down-regulation (red) for ≥50% of the genes, whereas light tone is for ≤50% of the genes

| Gene group | Ions vs control Up-regulated | Scaffolds vs control | Scaffolds vs ions | Ions vs control Down-regulated | Scaffolds vs control | Scaffolds vs ions |
|---|---|---|---|---|---|---|
| Bone matrix proteins | 0/4 | 2/4 | 2/4 | 2/4 | 2/4 | 1/4 |
| BMP superfamily | 4/11 | 7/11 | 6/11 | 1/11 | 1/11 | 3/11 |
| BMP receptors | 2/3 | 1/3 | 1/3 | 0/3 | 0/3 | 2/3 |
| Receptors | 1/11 | 3/11 | 2/11 | 4/11 | 6/11 | 3/11 |
| Growth factors | 1/10 | 0/10 | 1/10 | 5/10 | 6/10 | 2/10 |
| Integrin receptors | 3/5 | 4/5 | 2/5 | 1/5 | 1/5 | 0/5 |
| Collagen | 3/7 | 3/7 | 2/7 | 1/7 | 2/7 | 3/7 |
| Cartilage genes | 1/2 | 2/2 | 1/2 | 1/2 | 0/2 | 0/2 |
| Metalloproteinases | 2/4 | 2/4 | 0/4 | 2/4 | 1/4 | 1/4 |
| Transcription factors | 4/9 | 5/9 | 2/9 | 4/9 | 4/9 | 1/9 |
| Other genes | 2/11 | 3/11 | 4/11 | 4/11 | 5/11 | 1/11 |

*in vitro*.[45] A significant up-regulation of BMP2 indicates that the scaffolds and their ionic dissolution induced bone nodule formation and calcium deposition.

Additionally, scaffold induced significant up-regulation of BMP receptor type 1B (BMPR1B) related to the dissolution product group and the control; and dissolution products induced up-regulation of BMP receptor type 1A (BMP1A) and BMP receptor type II (BMPR2) without significant differences. During BMP pathway, the interaction of BMPR1A or BMPR1B and BMPR2 induces the phosphorylation of SMAD-1/5/8, necessary for the subsequent intracellular cascade activating osteoblast differentiation.[44] Also, SMAD3, an inhibitor of osteoblast differentiation, was down-regulated for all treatment groups without significant differences, suggesting that the material and ions not only induce osteogenesis but also disrupt cell processes that alter it.[41]

It was observed that hASCs cultured with the scaffolds and their dissolution products induced the up-regulation of integrin alpha 1 (ITGA1), integrin alpha 2 (ITGA2), and integrin beta 1 (ITGB1) (Table 2); these molecules are so much important in cellular adhesion between ECM and cells, and between material surface and cells as well as in cell communication.[47] When the integrins mediate adhesion between cells and ECM, cytoskeletal tension changes occur that induce different mechanochemical signal pathways that active osteoblast differentiation and initiate matrix mineralization.[21,36,48] Cell–matrix interactions mediated by integrins are vital in the regulation of osteoblast-specific gene expression and differentiation. Osteoblasts express several integrins, particularly integrin beta1 class, which performs an essential role in osteoblast differentiation.[37,49] Brunner et al. found the mechanism for the translocation of integrins B1 into fibrillar adhesions, which allows the correct fibronectin self-assembly into fibrils, vital for mineralization.[50] Table 4 shows that the scaffolds presented the highest ratio of up-regulated integrins and almost all of them showed significant differences. ITGA1 expression was significantly up-regulated in hASCs grown on the scaffolds, suggesting that the scaffold surface can stimulate the up-regulation of ITGA1. Olivares-Navarrete et al. found that ITGA1 was up-regulated in human MSCs grown on the microstructured titanium surfaces and the increase in ITGA1 expression was proportional to the surface roughness.[51] Moreover, the significant up-regulation of TGB1 suggests a tendency of the scaffolds to activate mineralization.

Collagen type I alpha 2 (COL1A2), collagen type XV alpha 1 (COL15A1), collagen type III alpha 1 (COL3A1), and collagen type V alpha 1 (COL5A1) were up-regulated in hASCs cultured with the scaffolds or the dissolution products without significant differences (Table 2). Collagens perform an important role in cell adhesion and can induce the release of several growth factors that are necessary for blood vessels, osteoclasts, and osteoblasts formation. Among them, collagen type I is the most abundant extracellular proteins in bone.[52,53] In our study, biglycan (BGN) expression was enhanced when hASCs were grown on the scaffold surface; BGN is an ECM proteoglycan that modulates osteoblast differentiation and matrix mineralization. Xu et al. found that BGN knockout mice presented deficient bone mass.[54] All things considered, up-regulation of collagens, FN1, and BGN in the scaffold group could suggest that matrix mineralization was favored in the scaffold group related to the control.[35] Nevertheless, these results were not statistically significant, indicating that hASCs grown on the scaffolds showed matrix mineralization comparable to that of the control. On the other hand, genes involved in collagen biosynthesis, such as, BMP1 and SSP1 were significantly up-regulated in hASCs grown on the scaffold surface, showing a tendency to activate matrix mineralization (Tables 2 and 3).[35] Despite these results, additional studies must be done to have better evidences about the potential of the scaffolds to activate matrix mineralization.

FGF2 is involved in the MSC stemness maintenance by keeping the cells in the noncommitted state during culture *in vitro* and has a great ability to stimulate proliferation; nevertheless, FGF2 could generate the reduction of mineralization genes.[45,55] Similarly, transforming growth factor beta (TGFB) induces osteoblast progenitor

enrichment and early differentiation but could inhibit mineralization at latter stage.[56] FGF2 and TGFB2 expressions were significantly down-regulated in hASCs grown on the scaffolds (Tables 2 and 3), suggesting that osteogenic promoters and antagonist genes reached an equilibrium that allowed adequate regulation of osteogenesis.[35] Also, fibroblast growth factor receptor 1 (FGFR1) was down-regulation in hASCs cultured with the scaffolds and the dissolution products (Table 2). This factor is up-regulated in early osteogenesis differentiation helping to promote osteogenesis differentiation; nevertheless, FGFR1 signaling in mature osteoblasts causes inhibition of mineralization.[57] Moreover, SP7 or osterix was down-regulated in hASCs for both groups (Table 2). Calabresa et al. found that the expression level of SP7 peaked during days 8–11 and diminished during matrix mineralization, this reduction is necessary to foster osteoblast differentiation in the late stage.[36] Zhu et al. found that SP7 is expressed by osteoblasts in mice during the differentiation process and is vital for their bone formation.[58] Nishimura et al. showed that SP7 is crucial for endochondral ossification and the formation of matrix vesicles; indeed, osterix deficiency mice presented no bone formation and the cartilage-matrix ossification was imperfect.[59]

SPP1 is vital for bone formation and can be produced during the whole osteogenic process, peaking around 4 weeks.[36] This factor is secreted by osteocytes, preosteoblasts, and osteoblasts and integrated into bone.[36] BGLAP or osteocalcin is the most common marker when the osteoblasts are totally differentiated; synthesis of this protein is carried out by mature osteoblasts before mineralization and it is deposited into osteoid.[26,60] During intramembranous ossification *in vitro*, BGLAP is down-regulated by osteocytes together with ALP and COL1; on the contrary, SPP1 is up-regulated.[61] In this study, BGLAP and ALP were significantly down-regulated in hASCs grown on the scaffolds, and COL1A1 and SPP1 showed no significant difference with the control. These results could suggest that on day 21, hASCs grown on the scaffolds had reached the complete maturation of osteoblasts, which are responsible for matrix deposition; and some of these osteoblasts embedded in the matrix become osteocytes.[61,62]

## 4 | CONCLUSIONS

hASCs cultured with the Biosilicate®/F18 glass (BioS-2P/F18) scaffolds or their dissolution products showed adequate cell viability and tolerated well the environment for up to 21 days. Moreover, all groups showed positive ALP activity that peaked at 14 day and was higher in hASCs grown on the scaffolds. Also, deposited calcium increased for 3 weeks. And on day 21, the dissolution product group showed a significantly higher amount of calcium than the control.

The scaffolds were tested and proven to promote osteogenic differentiation of human adipose-derived stem cells. We observed that the scaffold and the dissolution products were able to up-regulate different members of the bone matrix proteins, BMP superfamily, TGF superfamily receptor, transcription factors, integrin receptors, and collagens, which are essential for osteogenesis.

More genes involved in osteogenesis were significantly up-regulated in hASCs grown on the BioS-2P/F18 scaffold surface than in cells cultured with the dissolution products, indicating their higher potential to induce osteogenic differentiation. This is caused by scaffold topography and chemical composition, which induce cell growth and differentiation process. Gene expression of some factors, such as, BMP1, BMP2, and RUNX2, suggests that the osteogenic process is stimulated by the ions released by the biomaterial and the 3D interconnected porous scaffolds. RUNX2 was highly expressed in hASCs grown on the scaffolds; this factor is required for commitment of osteoprogenitors, proliferation, differentiation, and maintenance of the osteoblastic cells. Moreover, RUNX2 is targeted for several signaling pathways, such as, BMP, where BMP2 plays an important role. Additionally, BMP1 and BMP2 were significantly up-regulated in hASCs grown on the BioS-2P/F18 scaffold surface, inducing matrix development and mineralization. Similarly, genes, such as, FGFR1, FGF2, and TGFB2 that could inhibit mineralization were significantly down-regulation in hASCs grown on the scaffolds. Other studies must be done to determine if the BioS-2P/F18 scaffolds are more favorable towards matrix development and osteoblast differentiation than other bioactive materials.

This study showed that stem cells grown on the scaffolds synthesized with Biosilicate® glass–ceramic and bioactive glass F18 by the replica technique underwent proliferation, matrix deposition, and mineralization, demonstrating that the BioS-2P/F18 scaffolds have promising potential for bone tissue engineering and regenerative medicine applications.

## ACKNOWLEDGMENTS

This study was financed in part by the Coordination for the Improvement of Higher Education Personnel–Brazil (CAPES)–Finance Code 001. Moreover, this work was supported by Emerging Leaders in the Americas Program–Canada (ELAP), CNPq–Brazil, and São Paulo Research Foundation–Brazil (FAPESP)–Project number 2013/07793-6.

## REFERENCES

1. Liu Y, Lim J, Teoh SH. Review: development of clinically relevant scaffolds for vascularised bone tissue engineering. *Biotechnol Adv*. 2013;*31*(5):688-705.
2. Johnell O, Kanis JA. An estimate of the worldwide prevalence, mortality and disability associated with hip fracture. *Osteoporos Int*. 2004;*15*(11):897-902.
3. Stevens B, Yang Y, Mohandas A, Stucker B, Nguyen KT. A review of materials, fabrication methods, and strategies used to enhance bone regeneration in engineered bone tissues. *J Biomed Mater Res—Part B Appl Biomater*. 2008;*85*(2):573-582.
4. Gholipourmalekabadi M, Mozafari M, Gholipourmalekabadi M, et al. In vitro and in vivo evaluations of three-dimensional hydroxyapatite/silk fibroin nanocomposite scaffolds. *Biotechnol Appl Biochem*. 2015;*62*(4):441-450.
5. Hoppe A, Güldal NS, Boccaccini AR. A review of the biological response to ionic dissolution products from bioactive glasses and glass-ceramics. *Biomaterials*. 2011;*32*(11):2757-2774.
6. Dong C, Yonggang L. Application of collagen scaffold in tissue engineering: recent advances and new perspectives. *Polymers*. 2016;*8*(42):1-20.
7. Crovace MC, Souza MT, Chinaglia CR, Peitl O, Zanotto ED. Biosilicate®—a multipurpose, highly bioactive glass-ceramic. In vitro, in vivo and clinical trials. *J Non Cryst Solids*. 2016;*432*:90-110.

8. Renno ACM, Bossini PS, Crovace MC, Rodrigues ACM, Zanotto ED, Parizotto NA. Characterization and in vivo biological performance of biosilicate. *Biomed Res Int*. 2013;*2013*:1-7.
9. Hench LL, & Polak, JM. Third-generation biomedical materials. *Science*. 2002;*295*(5557):1014-1017.
10. Xynos ID, Hukkanen MVJ, Batten JJ, Buttery LD, Hench LL, Polak JM. Bioglass ®45S5 stimulates osteoblast turnover and enhances bone formation in vitro: implications and applications for bone tissue engineering. *Calcif Tissue Int*. 2000;*67*(4):321-329.
11. Ferraz EP, Oliveira FS, de Oliveira PT, et al. Bioactive glass-based surfaces induce differential gene expression profiling of osteoblasts. *J Biomed Mater Res Part A*. 2017;*105*(2):419-423.
12. Souza MT, Renno A, Peitl O, Zanotto E. New highly bioactive crystallization-resistant glass for tissue engineering applications. *Transl Mater Res*. 2017;*4*(1):014002.
13. Souza MT, Campanini LA, Chinaglia CR, Peitl O, Zanotto ED, Souza CWO. Broad-spectrum bactericidal activity of a new bioactive grafting material (F18) against clinically important bacterial strains. *Int J Antimicrob Agents*. 2017;*50*(6):730-733.
14. Passos TF, Souza MT, Zanotto ED, Souza CWO. Bactericidal activity and biofilm inhibition of F18 bioactive glass against *Staphylococcus aureus*. *Mater Sci Eng C*. 2020;*118*:111475.
15. Zuk P, Zhu M, Futrell JW, et al. Multilineage cells from human adipose tissue: implications for cell-based therapies. *Tissue Eng*. 2001;*7*(2):211-228.
16. Komarova S, Safranek L, Gopalakrishnan J, et al. Mathematical model for bone mineralization. *Front Cell Dev Biol*. 2015;*3*:1-11.
17. Selimović Š, Kaji H, Bae H, & Khademhosseini, A. Microfluidic systems for controlling stem cells microenvironments. *Microfluidic Cell Culture Systems*. 2nd ed. Oxford: William Andrew; 2012:192.
18. Born A, Rottmar M, Lischer S, et al. Correlating cell architecture with osteogenesis: first steps towards live single cell monitoring. *Eur Cells Mater*. 2009;*18*:49-62.
19. Anselme K. Osteoblast adhesion on biomaterials. *Biomaterials*. 2000;*21*:667-681.
20. Hakki SS, Bozkurt SB, Hakki EE. Osteogenic differentiation of MC3T3-E1 cells on different titanium surfaces. *Biomed Mater*. 2012;*7*:1-9.
21. Shen Y, Jing D, Hao J, Tang G, Yang P, Zhao Z. The effect of β-aminopropionitrile on skeletal micromorphology and osteogenesis. *Calcif Tissue Int*. 2018;*103*(4):411-421.
22. Yang X, Liu X, Huang Q, Zhang R. The stimulatory effect of silica nanoparticles on osteogenic differentiation of human mesenchymal stem cells. *Biomed Mater*. 2017;*12*:1-11.
23. Golub EE, Boesze-Battaglia K. The role of alkaline phosphatase in mineralization. *Curr Opin Orthop*. 2007;*18*(5):444-448.
24. Orimo H. The mechanism of mineralization and the role of alkaline phosphatase in health and disease. *J Nippon Med Sch*. 2010;*77*(1):4-12.
25. Panferov VG, Safenkova I, Varitsev YA, Zherdev A, Dzantiev BB. Enhancement of lateral flow immunoassay by alkaline phosphatase: a simple and highly sensitive test for potato virus X. *Microchim Acta*. 2018;*185*(1):1-9.
26. De Godoy RF, Hutchens S, Campion C, Blunn G. Silicate-substituted calcium phosphate with enhanced strut porosity stimulates osteogenic differentiation of human mesenchymal stem cells. *J Mater Sci Mater Med*. 2015;*26*(54):1-12.
27. Yu J, Xu L, Li K, et al. Zinc-modified calcium silicate coatings promote osteogenic differentiation through TGF-β/Smad pathway and osseointegration in osteopenic rabbits. *Sci Rep*. 2017;7:1-13.
28. Yang X, Li Y, Liu X, Huang Q, Zhang R, Feng Q. Incorporation of silica nanoparticles to PLGA electrospun fibers for osteogenic differentiation of human osteoblast-like cells. *Regen Biomater*. 2018;*5*:229-238.
29. Jones JR, Gentleman E, Polak J. Bioactive glass scaffolds for bone regeneration. *Elements*. 2007;*3*(6):393-399.
30. Mahdavi FS, Salehi A, Seyedjafari E, Mohammadi-Sangcheshmeh A, Ardeshirylajimi A. Bioactive glass ceramic nanoparticles-coated poly(L-lactic acid) scaffold improved osteogenic differentiation of adipose stem cells in equine. *Tissue Cell*. 2017;*49*(5):565-572.
31. Shu X, Feng J, Feng J, Huang X, Li L, Shi Q. Combined delivery of bone morphogenetic protein-2 and insulin-like growth factor-1 from nano-poly(γ-glutamic acid)/β-tricalcium phosphate-based calcium phosphate cement and its effect on bone regeneration in vitro. *J Biomater Appl*. 2017;*32*(5):547-560.
32. Atari M, Caballé-Serrano J, Gil-Recio C, Giner-Delgado C, Martínez-Sarrà E, García-Fernández DA. The enhancement of osteogenesis through the use of dental pulp pluripotent stem cells in 3D. *Bone*. 2012;*50*(4):930-941.
33. Bageshlooyafshar B, Vakilian S, Kehtari M, Eslami-Arshaghi T. Zinc silicate mineral-coated scaffold improved in vitro osteogenic differentiation of equine adipose-derived mesenchymal stem cells. *Res Vet Sci*. 2019;*124*:444-451.
34. Mendonça G, Mendonça DBS, Simo LGP, et al. The effects of implant surface nanoscale features on osteoblast-specific gene expression. *Biomaterials*. 2009;*30*:4053-4062.
35. Li J, Kawazoe N, Chen G. Gold nanoparticles with different charge and moiety induce differential cell response on mesenchymal stem cell osteogenesis. *Biomaterials*. 2015;*54*:226-236.
36. Calabrese G, Giuffrida R, Fabbi C, Figallo E, Furno D. Collagen-hydroxyapatite scaffolds induce human adipose derived stem cells osteogenic differentiation in vitro. *PLoS One*. 2016;*11*(3):1-17.
37. Xynos ID, Edgar AJ, Buttery LDK, Hench LL, Polak JM. Gene-expression profiling of human osteoblasts following treatment with the ionic products of bioglass 45S5 dissolution. *J Biomed Mater Res*. 2001;*55*(2):151-157.
38. Wang X, Jin T, Chang S, Zhang Z, Zajka-Jakubowska A, Nor JE. In vitro differentiation and mineralization of dental pulp stem cells on enamel-like fluorapatite surfaces. *Tissue Eng Part C*. 2012;*18*(11):821-830.
39. Kieswetter K, Schwartz Z, Hummert TW, et al. Surface roughness modulates the local production of growth factors and cytokines by osteoblast-like MG-63 cells. *J Biomed Mater Res*. 1996;*32*(1):55-63.
40. Anselme K, Bigerelle M, Noel B, et al. Qualitative and quantitative study of human osteoblast adhesion on materials with various surface roughnesses. *J Biomed Mater Res*. 2004;*49*(2):155-166.
41. Oliveira FS, Bellesini L, Defino HLA, da Silva Herrero CF. Hedgehog signaling and osteoblast gene expression are regulated by purmorphamine in human mesenchymal stem. *J Cell Biochem*. 2012;*113*:204-208.
42. Chen Q, Shou P, Zheng C, et al. Fate decision of mesenchymal stem cells: adipocytes or osteoblasts? *Cell Death Differ*. 2016;*23*:1128-1139.
43. Haque T, Hamade F, Alam N, et al. Characterizing the BMP pathway in a wild type mouse model of distraction osteogenesis. *Bone*. 2008;*42*:1144-1153.
44. Castro-Raucci LMS, Francischini MS, Teixeira LN, et al. Titanium with nanotopography induces osteoblast differentiation by regulating endogenous bone morphogenetic protein expression and signaling pathway. *J Cell Biochem*. 2016;*117*:1718-1726.
45. Mareddy S, Dhaliwal N, Crawford R, Xiao Y. Stem cell–related gene expression in clonal populations. *Tissue Eng Part A*. 2010;*16*(2):749-759.
46. Herzog E, Dohle E, Bischoff I, Kirkpatrick CJ. Cell communication in a coculture system consisting of outgrowth endothelial cells and primary osteoblasts. *Biomed Res Int*. 2014;*2014*:1-15.
47. Minaříková M, Oralová V, Veselá B, Radlanski R. Osteogenic profile of mesenchymal cell populations contributing to alveolar bone formation. *Cells Tissues Organs*. 2015;*200*:339-348.
48. Schneider GB, Zaharias R, Stanford C. Osteoblast integrin adhesion and signaling regulate mineralization. *J Dent Res*. 2001;*80*(6):1540-1544.

49. Marie PJ. Bone cell–matrix protein interactions. *Osteoporos Int*. 2009;*20*:1037-1042.
50. Brunner M, Millon-frémillon A, Chevalier G, et al. Osteoblast mineralization requires B1 integrin/ICAP-1–dependent fibronectin deposition. *J Cell Biol*. 2011;*194*(2):307-322.
51. Olivares-Navarrete R, Hyzy SL, Hwa J, et al. Mediation of osteogenic differentiation of human mesenchymal stem cells on titanium surfaces by a Wnt-integrin feedback loop. *Biomaterials*. 2011;*32*(27):6399-6411.
52. Xue Y, Xing Z, Hellem S, Arvidson K, Mustafa K. Endothelial cells influence the osteogenic potential of bone marrow stromal cells. *Biomed Eng Online*. 2009;*8*:1-9.
53. Grassi F, Cattini L, Gambari L, et al. T cell subsets differently regulate osteogenic differentiation of human mesenchymal stromal cells in vitro. *J Tissue Eng Regen Med*. 2016;*10*:305-314.
54. Xu T, Bianco P, Fisher LW, et al. Targeted disruption of the biglycan gene leads to an osteoporosis-like phenotype in mice. *Nat Genet*. 1998;*20*:78-82.
55. Hughes-Fulford M, Li C-F. The role of FGF-2 and BMP-2 in regulation of gene induction, cell proliferation and mineralization. *J Orthop Surg Res*. 2011;*6*:1-8.
56. Wu M, Chen G, Li YP. TGF-β and BMP signaling in osteoblast, skeletal development, and bone formation, homeostasis and disease. *Bone Res*. 2016;*4*:16009.
57. Long F. Building strong bones: molecular regulation of the osteoblast lineage. *Nat Rev Mol Cell Biol*. 2012;*13*(1):27-38.
58. Zhu F, Friedman MS, Luo W, Woolf P, Hankenson KD. The transcription factor osterix (SP7) regulates BMP6-induced human osteoblast differentiation. *J Cell Physiol*. 2012;*227*(6):2677-2685.
59. Nishimura R, Wakabayashi M, Hata K, et al. Osterix regulates calcification and degradation of chondrogenic matrices through matrix metalloproteinase 13 (MMP13) expression in association with transcription factor Runx2 during endochondral ossification. *J Biol Chem*. 2012;*287*(40):33179-33190.
60. Zan X, Sitasuwan P, Feng S, Wang Q. Effect of roughness on in situ biomineralized CaP-collagen coating on the osteogenesis of mesenchymal stem cells. *Langmuir*. 2016;*32*:1808-1817.
61. Franz-Odendaal TA, Hall BK, Witten PE. Buried alive: how osteoblasts become osteocytes. *Dev Dyn*. 2006;*235*(1):176-190.
62. Rutkovskiy A, Stensløkken K-O, Vaage IJ. Osteoblast differentiation at a glance. *Med Sci Monit Basic Res*. 2016;*22*:95-106.


**How to cite this article:** Marin CP, Santana GL, Robinson M, Willerth SM, Crovace MC, Zanotto ED. Effect of bioactive Biosilicate®/F18 glass scaffolds on osteogenic differentiation of human adipose stem cells. *J Biomed Mater Res*. 2021;109:1293–1308. https://doi.org/10.1002/jbm.a.37122